

## CONTACT STRESSES AND DEFORMATIONS IN THRUST BALL BEARING

Tatjana LAZOVIĆ<sup>1,\*</sup> - Sanja VARAGIĆ<sup>2</sup> - Ljubica MILOVIĆ<sup>3</sup>

<sup>1</sup> University of Belgrade, Faculty of Mechanical Engineering, Belgrade, Serbia

<sup>2</sup> ATB SEVER, Subotica, Serbia

<sup>3</sup> University of Belgrade, Faculty of Technology and Metallurgy, Belgrade, Serbia

*Received* (05.05.2018); *Revised* (04.06.2018); *Accepted* (06.06.2018)

**Abstract:** The aim of this paper is to determine deformations and stresses in the statically loaded thrust ball bearing subjected to a centric external axial load. In this case, all balls in the bearing are equally engaged in the transmission of the operational load. The influence of the load on the stresses and deformations in the bearings of different series has been analysed. The obtained results are the basis for further research of the load distribution in an eccentrically loaded axial ball bearing in order to determine the reduction of the static load bearing capacity in relation to the values determined in appropriate standard and also to the values prescribed by manufacturers' catalogues.

**Key words:** thrust ball bearing, load distribution, contact stress, contact deformation.

### 1. INTRODUCTION

The thrust ball bearings are designed to bear the axial load of shafts or axles in mechanical systems where axial load predominate such as the ship propeller, machine tool tables and spindles, ball screws, fluid control valves, oil and gas rotary tables [1,2]. Standard recommendations for determining the static and dynamic load rating [3,4] are considered for centrally loaded thrust ball bearings. In this case, the load distribution between rolling elements in the bearing is equal. In [5-8], authors consider tribological phenomena and energy loss conditions in thrust ball bearing, under the equal load distribution. The load is equally distributed between all balls in the thrust ball bearing of ideal geometry and centrally loaded by pure external axial force. This is the ideal and most comfortable case of the thrust bearing loading. However, in reality, the load distribution is unequal, more or less, depending on the position of the external axial load, the stiffness of the contacting bearing parts (balls and raceways) and of the bearing internal geometry [9]. In eccentrically loaded thrust bearing, an additional load in the form of a tilting moment occurs, as well [10]. The influence of the tilting moment on the load distribution between the balls and the service life of the thrust ball bearing was analysed in [11]. The degree of inequality of the load distribution in the bearing influences its dynamic behaviour, friction and wear processes, as well as the service life [12-14]. An analysis of the stresses and deformations in the centrally loaded thrust ball bearing was carried out in this paper. A case of equal load distribution is considered, as a base for further analyses of inequally loaded thrust ball bearing conditions.

### 2. THRUST BALL BEARING GEOMETRY

The thrust ball bearing external geometry is determined by international standards. The internal geometry is determined by the manufacturers in accordance with their

technological processes, and based on the results of the optimization carried out in the development of the bearing construction, in order to obtain better performance. For each standard bearing, with the same external (standard) dimensions, different variants of internal dimensions are possible. All these bearing parts' dimensions combinations must be made in a certain available space, depending on standard external geometry. In the thrust ball bearings, this space is limited by height  $H$  and width  $(D - d)/2$  (Figure 1). The external dimension of single row (one direction) thrust ball bearing prescribed by appropriate standard [15] are (Figure 1):  $d$  - bore diameter of shaft washer;  $d_1$  - outer diameter of shaft washer;  $D_1$  - bore diameter of housing washer;  $D$  - outer diameter of housing washer;  $H$  - bearing height;  $r$  - washer fillet radius.

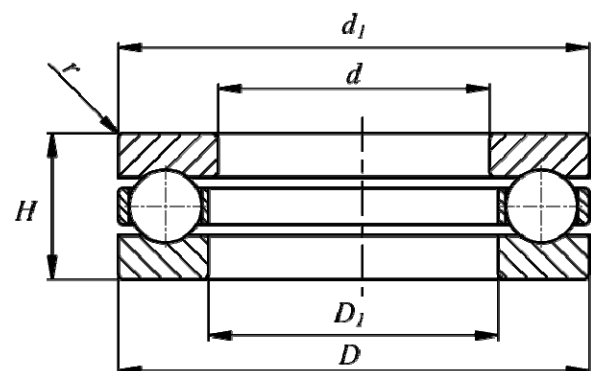


Fig.1. Outer dimensions of the thrust ball bearing

The internal thrust ball bearing geometry is determined by the dimensions of the raceways, balls, and cage. It affects the load distribution between balls, stresses and deformations, friction moment, vibrations, noise generation, static and dynamic load carrying capacity. There are no standards for internal bearing geometry that contain data and guidelines for shapes and dimensions. Based on previous stress calculations, contact

\* Correspondence Author's Address: University of Belgrade, Faculty of Mechanical Engineering, Kraljice Marije 16, 11000 Belgrade, Serbia, tlazovic@mas.bg.ac.rs

deformations, load distribution between balls and bearing service life, manufacturers determine the diameter and number of balls, raceways radii, chamfers and fillets, as well as relations between these geometric parameters, using suitable optimization methods.

The raceways have the toroid shape defined by two dimensions: the radius of the torus cross-section or radius of the torus tube and the radius of the torus i.e. distance between the centre of the torus tube and the centre of the torus. The rolling elements have the shape of the sphere (balls). They are arranged in the bearing workspace with equal angle distance (Figure 2).

The basic internal dimensions of the thrust ball bearing are (Figure 2):  $d, D_1$  – bore diameter of the shaft/housing washer;  $d_1, D$  – outer diameter of the shaft/housing washer;  $h, h_1$  – shaft/housing cage height;  $D_0, D_{01}$  – raceway diameter of the shaft/housing washer;  $R, R_1$  – raceway's groove radius of the shaft/housing washer;  $h_0, h_{01}$  – raceway depth of the shaft/housing washer;  $t_0, t_{01}$  – raceway width of the shaft/housing washer;  $r$  – fillet radius;  $D_w$  – ball diameter;  $\gamma$  – angle between balls;  $D_p$  – pitch diameter (equal to raceway diameter).

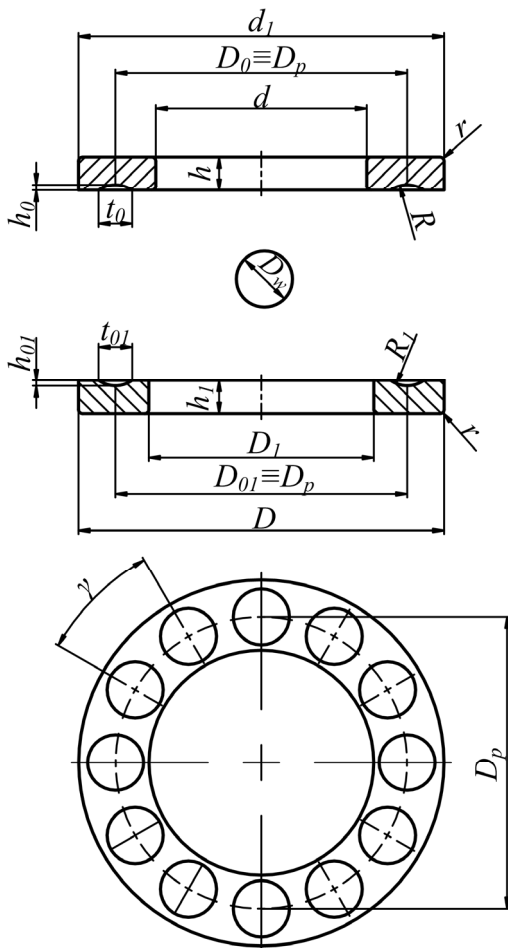


Fig.2. The internal geometry of thrust ball bearing

Axial ball bearings of different series (511, 512, 513 and 514) and the same bore diameter are shown in Figure 3. These bearings have different height  $H$ , outer diameter  $D$  and diameter of the balls  $D_w$ . The number of balls in the bearings of different series is different and decreases with the increase in the series.

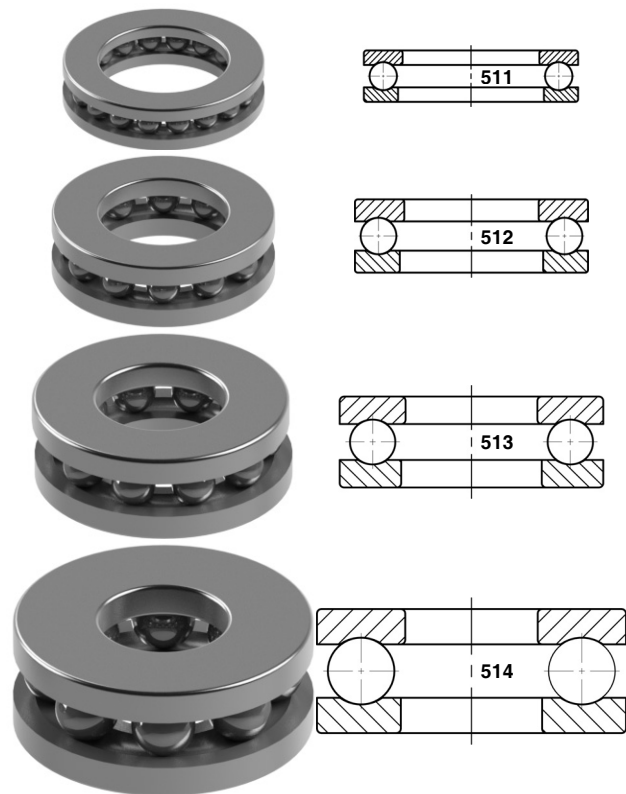


Fig.3. Thrust ball bearings of different series (511, 512, 513 u 514) and the same bore diameter

### 3. CONTACT STRESSES AND DEFORMATIONS

In the unloaded thrust ball bearing, rolling elements – balls contact with raceways of toroid shape. Transferring the load between washers, the balls and raceways are deformed, so that contacting occurs on the small surfaces of the ellipse shape (Fig. 4 and 5). The size of the contact ellipse depends on the material elastic properties, the contact surfaces curvature and on the load transferred by balls.

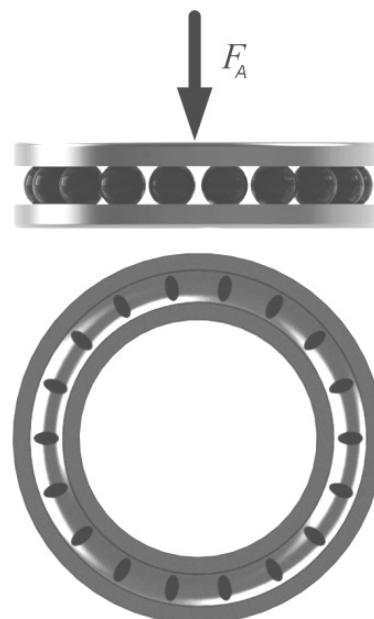


Fig.4. Contact ellipses in thrust ball bearing

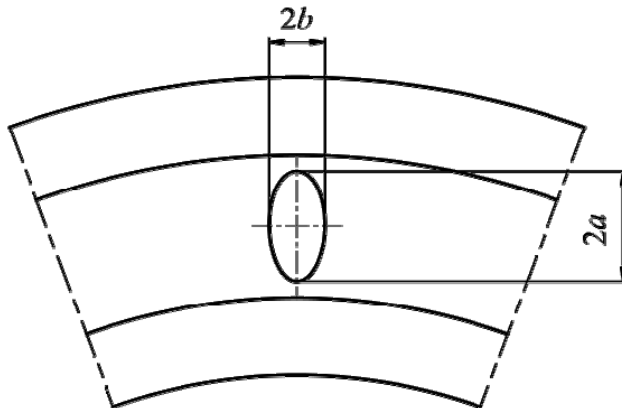


Fig.5. Dimensions of contact ellipse

Contact stresses and deformations in contact between the balls and the raceways of the thrust ball bearing can be determined using the *Hertz* theory. In accordance with this theory, the dimensions (semi-major and semi-minor axis) of the contact ellipse (Figure 5) are [1,2]:

$$a = n_a \left( \frac{3(1-\nu^2)F}{E \sum \rho} \right)^{1/3}; \quad b = n_b \left( \frac{3(1-\nu^2)F}{E \sum \rho} \right)^{1/3} \quad (1)$$

where:

- $a$  - semi-major axis of the contact ellipse;
- $b$  - semi-minor axis of the contact ellipse;
- $F$  - normal force in contact;
- $E$  - *Young's* modulus of the contacting bearing parts (balls and raceways);
- $\nu$  - *Poisson's* ratio;
- $\sum \rho$  - sum of the contact surfaces curvatures;
- $n_a, n_b$  - parameters of the elliptic integrals according to [1,2].

The sum of the contact surfaces curvatures in (1) can be expressed as [1,2]:

$$\sum \rho = \rho_{11} + \rho_{12} + \rho_{21} + \rho_{22} = \frac{1}{R_{11}} + \frac{1}{R_{12}} + \frac{1}{R_{21}} + \frac{1}{R_{22}} \quad (2)$$

where  $R_{11}, R_{12}, R_{21}$  and  $R_{22}$  are radii of contact surfaces in two perpendicular cross-sections of the contact (Figure 6). Based on dimensions given in Figures 2 and 6, the expression (2) can be written in the following form [5]:

$$\sum \rho = \frac{2}{R_w} - \frac{1}{R} \quad (3)$$

where  $R_w$  and  $R$  are radii of the balls and raceway groove, respectively.

By substitution (3) in (1), the semi-major and semi-minor axes of the contact ellipse of the thrust ball bearing are obtained:

$$a = n_a \left( \frac{3(1-\nu^2)FD_w}{2E(2-\xi)} \right)^{1/3}; \quad b = n_b \left( \frac{3(1-\nu^2)FD_w}{2E(2-\xi)} \right)^{1/3} \quad (4)$$

where  $\xi = R_w/R$ ;  $D_w = 2R_w$  is ball diameter (Figure 2).

The parameters  $n_a$  and  $n_b$  from (1) and (4) are determined using the tables or diagrams [9,10] depending on auxiliary

function  $\cos \tau$  which is different for different types of rolling bearings. In the case of thrust ball bearings, this function is:

$$\cos \tau = \frac{D_w}{4R - D_w} = \frac{\xi}{2 - \xi} \quad (5)$$

Maximal contact stress between balls and raceways in the middle of the contact ellipse (Figure 7) is [1,2]:

$$\sigma_{\max} = \frac{3}{2} \cdot \frac{F}{\pi ab} \quad (6)$$

Contact deformation of balls and raceways can be determined based on expression [1,2]:

$$\delta = C_F F^{2/3} \quad (7)$$

The constant  $C_F$  in (7) depends on bearing internal geometry and on material properties of the contacting bearing parts (balls and raceways). In the case of thrust ball bearing made of steel [1,2]:

$$C_F = \left( \frac{2K}{\pi n_a} \right) \sum \rho^{1/3} \cdot 10^{-5} \frac{\text{mm}}{\text{N}^{2/3}} \quad (8)$$

where  $2K/\pi n_a$  is the auxiliary value given in tables or diagrams [9,10], depending on function  $\cos \tau$ .

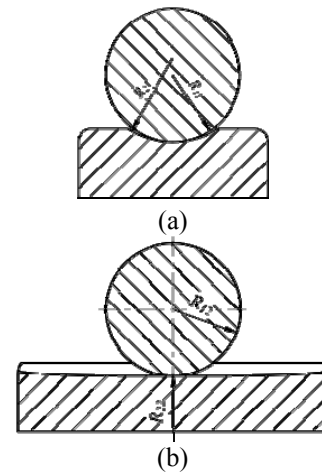


Fig.6. Cross section of contact surfaces along the contact ellipse axes: a) semi-major  $a$ ; b) semi-minor  $b$

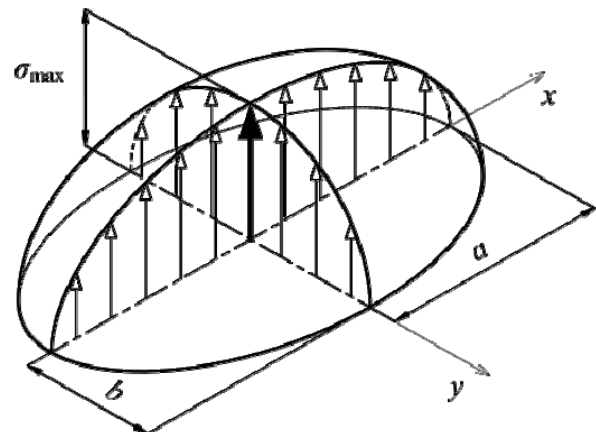


Fig.7. Stress distribution on contact ellipse

If the thrust ball bearing is loaded with an axial force acting in the direction of the bearing axis (centrally loaded bearing) then the total external load is equally distributed to all balls in the bearing (Figure 8):

$$F_i = \frac{F_A}{z}, \quad i = 0 \dots z-1, \quad (9)$$

where  $F_i$  is normal load in contact between ball and raceway and  $z$  is a number of balls in the bearing.

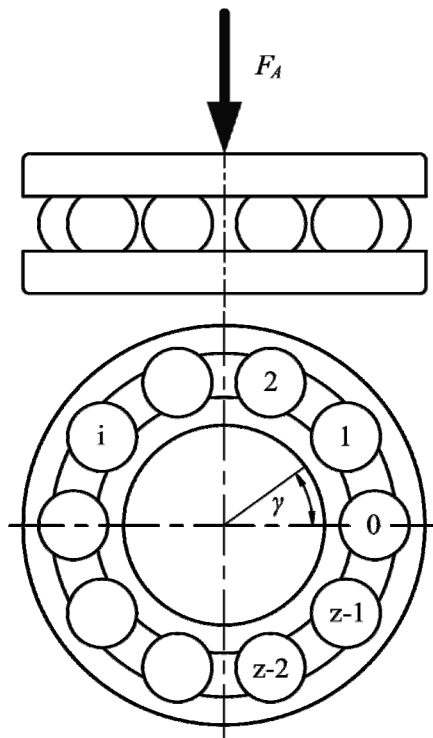


Fig.8. Centrally loaded thrust ball bearing with  $z$  balls

Table 1. Properties of the thrust ball bearings of bore diameter 30 mm

Quantity		511	512	513	514
Bore diameter, mm	$d$		30		
Outside diameter, mm	$D$	47	52	60	70
Height, mm	$H$	11	16	21	28
Number of balls	$z$	18	12	10	8
Ball diameter, mm	$D_w$	6.00	7.98	10.30	15.10
Angle between balls, °	$\gamma$	20	30	36	45
Raceway diameter, mm	$D_0$	38.5	41.5	45.0	50.0
The ratio of the balls and raceway groove radii	$\xi$		0,93		
Raceway groove radius, mm	$R$	3.23	4.29	5.54	8.12
Static load rating, kN	$C_0$	43	51	65	122
Dynamic load rating, kN	$C$	19	25.5	35.8	70.2
Poisson's ratio:	$\nu$		0.3		
Young's modulus of the steel, N/mm <sup>2</sup>	$E$		$2.1 \cdot 10^5$		

In the statically loaded thrust ball bearing, when the relative rotational speed of the bearing washers is  $n \leq 10$  rpm, the normal load in contact between ball and raceway from (9) can be expressed as a function of the static bearing load carrying capacity:

$$F_i = \frac{C_0}{z} k_F, \quad i = 0 \dots z-1, \quad (10)$$

where:  $C_0$  is static load rating (bearing property, given in the manufacturer's catalogues);  $k_F = F_A/C_0$  is the relative load.

Based on (8) and (5), the expressions for contact ellipse semi-axes (4), the maximal contact stress between the balls and the raceways (6) and the total contact deformation of the ball and the raceways (7) can be written in the following form, respectively:

$$a = n_a \left( \frac{3(1-\nu^2)D_w C_0}{2E(2-\xi)z} k_F \right)^{1/3}; \quad (11)$$

$$b = n_b \left( \frac{3(1-\nu^2)D_w C_0}{2E(2-\xi)z} k_F \right)^{1/3}$$

$$\sigma_{\max} = \frac{3}{2} \frac{C_0}{\pi abz} k_F \quad (12)$$

$$\delta = C_F \left( \frac{C_0 k_F}{z} \right)^{2/3} \quad (13)$$

#### 4. A NUMERICAL EXAMPLE AND DISCUSSION

Based on previous considerations, an analysis of stresses and deformations in thrust ball bearings with bore diameter  $d = 30$  mm of all standard series: 511, 512, 513 and 514 (Figure. 3) is obtained. The basic information on these bearings is given in Table 1.




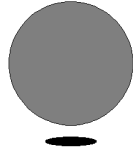
Four cases of the bearing loading were analyzed, with an external axial load of (25, 50, 75 and 100)% of the bearing static load carrying capacity. The auxiliary values  $\cos\tau$  and  $2K/\pi n_a$  are determined using available data on the internal bearing geometry (the balls diameter  $D_w$  and radius of raceway groove radius  $R$ ). Semi-major and semi-minor axes of the contact ellipse, contact stresses and contact deformations are determined using (9), (10) and (11). The results are shown in Table 2.

Table 2. Dimensions of the contact ellipses, normal contact load, and stresses and deformations of the balls and raceways depending on the external axial load of the all standard series of the thrust ball bearings with bore diameter 30 mm

Quantity, unit		511	512	513	514	
	$\cos\tau$			0.87		
	$n_a$			2.77		
	$n_b$			0.49		
	$2K/\pi n_a$			0.721		
	$C_F, 10^{-6} \text{ mm/N}^{2/3}$	5.1	4.6	4.2	3.7	
$k_F$	0.25	$F_i, 10^3 \text{ N}$	0.60	1.06	1.62	3.81
		$a, \text{ mm}$	0.733	1.031	1.293	1.952
		$b, \text{ mm}$	0.137	0.182	0.229	0.345
		$\sigma_{\max}, \text{ N/mm}^2$	2695	2700	2624	2702
		$\delta, \text{ mm}$	0.0003	0.0005	0.0006	0.0009
	0.50	$F_i, 10^3 \text{ N}$	1.20	2.12	3.25	7.62
		$a, \text{ mm}$	0.974	1.299	1.629	2.459
		$b, \text{ mm}$	0.172	0.230	0.288	0.435
		$\sigma_{\max}, \text{ N/mm}^2$	3395	3402	3306	3404
		$\delta, \text{ mm}$	0.0006	0.0008	0.0009	0.0014
	0.75	$F_i, 10^3 \text{ N}$	1.79	3.19	4.88	11.44
		$a, \text{ mm}$	1.115	1.486	1.865	2.815
		$b, \text{ mm}$	0.197	0.263	0.33	0.498
		$\sigma_{\max}, \text{ N/mm}^2$	3887	3894	3785	3897
		$\delta, \text{ mm}$	0.0007	0.0010	0.0012	0.0019
	1.00	$F_i, 10^3 \text{ N}$	2.39	4.25	6.50	15.25
	$a, \text{ mm}$	1.228	1.636	2.052	3.098	
	$b, \text{ mm}$	0.217	0.289	0.363	0.548	
	$\sigma_{\max}, \text{ N/mm}^2$	4278	4286	4165	4289	
	$\delta, \text{ mm}$	0.0009	0.0012	0.0015	0.0023	

A comparative illustration of the balls and contact ellipses for these four cases is given in Table 3.

Table 3. Balls and contact ellipses dimensions ( $F_A = C_0$ )

Bearing	511	512	513	514
Ball and related contact ellipse				
$D_w$ , mm	6.00	7.98	10.30	15.10
$a$ , mm	1.228	1.636	2.052	3.098
$b$ , mm	0.217	0.28	0.363	0.548

Based on data from the Tables 2 and 3, the diagrams shown in Figures 9-11 are drawn.

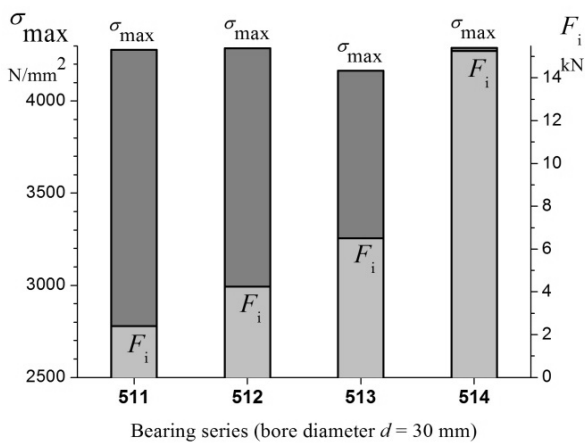


Fig.9. Contact stress and normal load between balls and raceways

element/raceway. The contact stress values are: 4600 MPa for self-aligning ball bearings, 4200 MPa for all other ball bearings and 4000 MPa for all roller bearings. In the case of thrust ball bearings, this stress value is 4200 MPa. The diagrams in Figures 9 and 10 relate to bearings loaded by the maximum external axial load equal to static load rating, when the relative load is  $k_F = 1$  (Table 1).

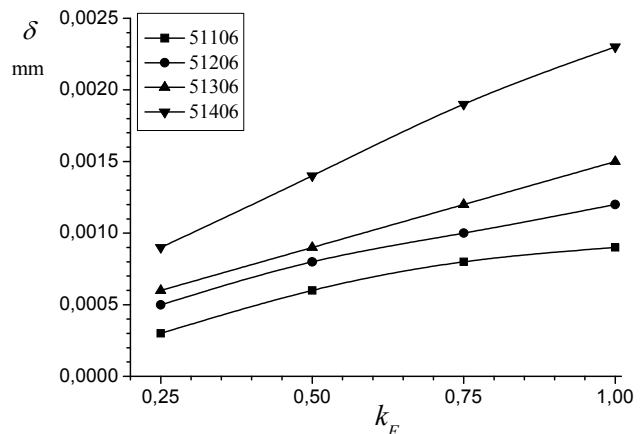


Fig.11. Contact deformation of ball and raceway depending on external load

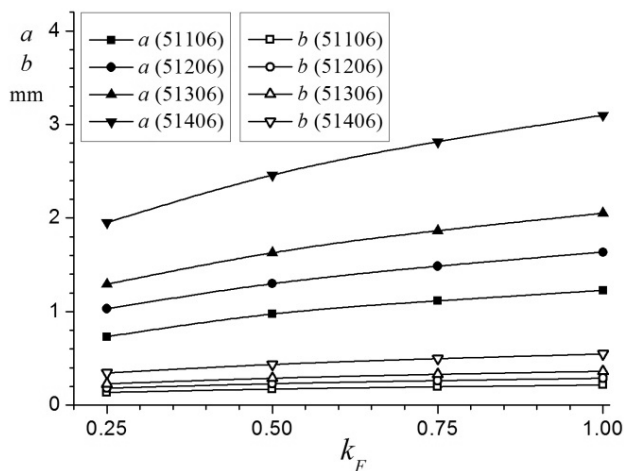


Fig.10. Contact ellipse dimensions depending on external load

The basic static load rating  $C_0$  is defined in ISO 76 [3] as the load that results in a certain value of contact stress at the centre of contact of the most heavily loaded rolling

Comparing the bearings of different series, from light to heavy one, the load of balls is increased (Figure 9), but the maximum stress at contact of balls and raceways is approximately the same for all series. This is caused by increase in contact ellipse (Figure 10) due to the increasing the dimensions of the balls and the raceways (Tables 2 and 3). When bearings are loaded with an external centric axial load equal static load rating, the stresses are within the limits (4165...4289) MPa. The relative deviations are  $(2 \pm 1)\%$ , that can be tolerated, and is caused by the different internal geometry of the bearings. With the load increase, the contact deformations of the balls and the raceways are also increased. The contact deformations determined by (13) are shown in the diagrams in Figure 11. It can be noticed that the deformations corresponding to the load equal to static load rating and the stress determined by the standard definition of static load rating

(4200 MPa) are larger than the standardized values of  $10^{-4}$  of balls diameter [3]. The cause could be the different internal bearing geometry (balls and raceways dimensions) and the conventional *Hertz* theory applied. More accurate analysis of contact deformations can be made using appropriate experimental or numerical methods. Contact stresses and deformations were determined using the conventional *Hertz* theory in the case of a centrally loaded axial bearing [1,2]. In addition, the maximum operational load equal to static load rating corresponds to the standard defined stress at contact between balls and raceways of 4200 MPa. However, in the case of an eccentrically loaded bearing (Figure 12), the load distribution between the balls is unequal. One or more balls in the bearing are loaded with a force greater than  $F_A/z$ . This means that the contact stress will be larger than the value defined in standard. ISO standard [3] does not consider eccentrically loaded thrust ball bearings.

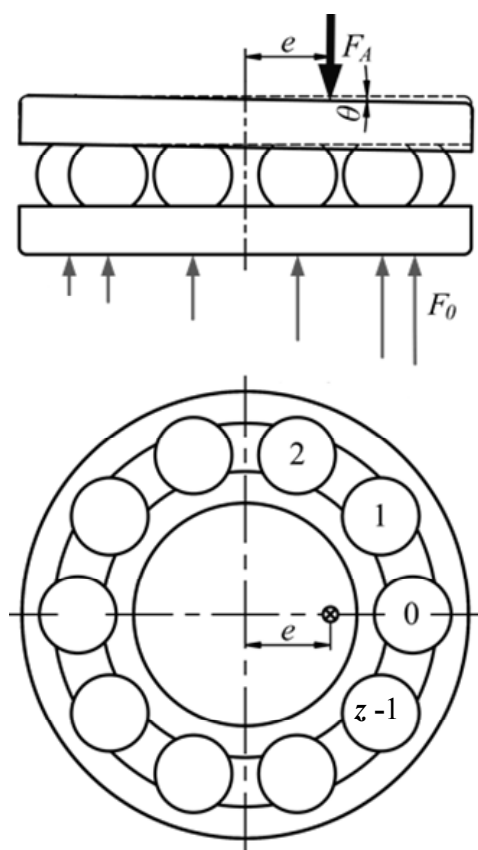


Fig.12. Eccentrically loaded bearing with  $z$  balls

## 5. CONCLUSION

The analyzes carried out are the basis of further research of the thrust ball bearing load carrying capacity under the condition of an eccentric external axial load, i.e. unequal load distribution between balls. In this case, the contact stress of the most heavily loaded ball may be larger than the limit value and can cause unforeseen premature and excessive damage of the bearing. Results can be used for more exact prediction of the thrust ball bearing load carrying capacity in operation, as well as in case studies for failure analysis [16,17].

## ACKNOWLEDGEMENTS

This work has been performed within the projects TR35011 and TR35029, supported by the Serbian Ministry of Education, Science and Technological Development, which financial help is gratefully acknowledged.

## REFERENCES

- [1] Harris T A 1984 *Rolling Bearing Analysis*, John Wiley and Sons, New York
- [2] Harris T and Kotzalas M 2006 *Advanced Concepts of Bearing Technology*, Taylor & Francis Group, London - New York
- [3] ISO 76:1987 *Rolling bearings – Static load ratings*, International Organization for Standardization
- [4] ISO 281:1990 *Rolling bearings – Dynamic load ratings and rating life*, International Organization for Standardization
- [5] Ren Z, Wang J, Guo F and Lubrecht A A 2014 Experimental and numerical study of the effect of raceway waviness on the oil film in thrust ball bearings, *Tribology International*, 73 1-9
- [6] Cousseau T, Graça B, Campos A and Seabra J 2011 Friction torque in grease lubricated thrust ball bearings, *Tribology International*, 44 523-531
- [7] Cousseau T, Graça BM, Campos A V and Seabra J H O 2012 Influence of grease rheology on thrust ball bearings friction torque, *Tribology International*, 46 106-113
- [8] Fernandez C M C, Marques P M T, Martins R and Seabra J H O 2015 Gearbox power loss. Part I: Losses in rolling bearings, *Tribology International*, 88 298-308
- [9] Ristivojević M and Mitrović R 2002 *Load distribution – Gears and rolling bearings* (in Serbian), Faculty of Mechanical Engineering, University of Belgrade
- [10] Varagić S 2014 *Operational ability of statically loaded thrust ball bearing* (in Serbian), Faculty of Mechanical Engineering, University of Belgrade, Serbia, M.Sc. Thesis
- [11] Tianyu L and Jiwei L 2012 *The influence of moment load on fatigue life of thrust ball bearing*, International Conference on Mechanical Engineering and Material Science - MEMS, Shanghai, China, Dec. 28-30, pp. 25-28
- [12] Lazovic T, Ristivojevic M and Mitrovic R 2008 Mathematical model of load distribution in rolling bearing, *FME Transactions*, 36 189-196
- [13] Lazović T 2014 *Abrasive wear of rolling bearings* (in Serbian), Faculty of Mechanical Engineering, University of Belgrade
- [14] Lazovic T, Mitrovic R and Ristivojevic M 2010 Influence of internal radial clearance on the ball bearing service life, *Journal of the Balkan tribological association*, 16 (1) 1-8

- [15] ISO 104:2015 *Rolling bearings – Thrust bearings – Boundary dimensions, general plan*, International Organization for Standardization
- [16] Marinković A, Lazović T, Milović Lj and Marković S 2015 *Contact stress and deformations in thrust ball bearings for heavy machinery excavators*, XXI International Conference on „Material Handling, Constructions and Logistics“ – MHCL, Vienna, Austria, Sep. 23-25, pp. 123-128
- [17] Marinković A, Lazović T, Grbović A, Stanković M and Minewitsch A 2016 *Contact stress study and FME analysis of large size thrust ball bearings*, 5th International Conference on Power Transmission BAPT, Ohrid, Oct. 5-8, pp. 7-14

